Using an LU Recombination Method to Improve the Performance of the Boundary Element Method at Very Low Frequencies

Haixin Ke   and   Todd H. Hubing

Electromagnetic Compatibility Laboratory
Department of Electrical and Computer Engineering
University of Missouri-Rolla
Rolla, MO 65409
hkm6b@umr.edu

Abstract— **Many numerical electromagnetic modeling techniques that work very well at high frequencies do not work well at lower frequencies. This is directly or indirectly due to the weak coupling between the electric and magnetic fields at low frequencies. One technique for improving the performance of boundary element techniques at low frequencies is through the use of loop-tree basis functions, which decouple the contributions from the vector and scalar electric potential. However, loop-tree basis functions can be difficult to define for large, complex geometries. This paper describes a new method for improving the low-frequency performance of boundary element techniques. The proposed method does not require special basis functions and is relatively easy to implement. Numerical errors introduced by the great difference in scale between the vector and scalar electric potential are corrected automatically during the LU decomposition of the impedance matrix.**

Keywords-EFIE;low frequency; MOM

I. INTRODUCTION

The boundary element method is a widely used numerical electromagnetic modeling technique. Boundary element modeling codes use the method of moments to solve an electric field integral equation (EFIE) or magnetic field integral equation (MFIE) to calculate the equivalent currents induced on a surface in the presence of an exciting field. There are many boundary element modeling codes available that do an excellent job of modeling complex geometries at high frequencies (megahertz and higher). At low frequencies however, these codes may exhibit instabilities, particularly when using general purpose basis functions such as the popular Rao-Wilton-Glisson (RWG) [1] basis functions [2, 3, 4]. These instabilities can be explained in terms of the natural Helmholtz decomposition of Maxwell's equations [5]. At low frequencies, the magnetic vector potential and the electric scalar potential become more decoupled. Their representations in the impedance matrix become heavily unbalanced [3, 6] and this unbalance results in the loss of important information due to the finite precision of the numerical computations.

Loop-tree basis functions have been proposed to overcome this difficulty [3]. These basis functions allow the divergence-free and the curl-free components of the current, which have different frequency dependencies, to be separated [5]. The round-off error due to the difference in size of the scalar and vector potential contributions is avoided. Unfortunately, loop-tree basis functions are not widely used because they can be difficult to work with; particularly if the geometry being modeled is large and complex.

In this paper we present a new method for addressing the low frequency problem with boundary element techniques. This method is based on the fact that loop-tree basis functions can be formed from linear combinations of RWG basis functions. The new method performs similar linear combinations mathematically, without explicitly defining new basis functions. Thus, it can be easily applied to existing boundary element algorithms.

The rest of the paper is organized as follows: Section II describes how boundary elements methods break down at low-frequencies; Section III gives a brief description of loop-tree basis function method; Section IV describes the new LU recombination method and its relationship to the loop-tree method; Section V presents a numerical example; and finally in Section VI, we provide a brief summary.

II. LOW-FREQUENCY PROBLEM

Consider the electromagnetic scattering from perfect electric conductors (PECs). The "mixed-potential" form of the EFIE for scattering problems is expressed as

$$\mathbf{E}^{sca} = -j\omega\mathbf{A} - \nabla\Phi \ . \tag{1}$$

The first term on the right-hand side of this equation is directly proportional to frequency while the second term is inversely proportional to frequency. When the frequency goes low enough so that the size of the scatterer becomes small compared to the wavelength, the contribution of the electric scalar potential, Φ, dominates that of the vector potential, $\mathbf{A}$.

The low frequency problem can be understood more clearly by examining the testing process [7]. A vector identity states that the integration of the gradient $\nabla\Phi$ is path-independent. If the scatterer geometry is such that the current density can flow in closed loops, the testing of the scalar potential associated with the loops are not independent. So at low frequencies, where the scalar potential dominates the vector potential, the rank of the MOM matrix collapses. If for any reason the scalar potential cannot be accurately evaluated, the error will overwhelm the information from the vector potential and the solution to the matrix equation will be unstable.

A square loop example was created to demonstrate the low frequency problem while using the method of moments to solve the EFIE. The geometry of the loop is shown in Fig. 1. At low frequencies, this geometry can be modeled as a lumped circuit with a resistor and an inductor in series so that the current on the resistor can be calculated. Fig. 2 compares the full-wave solution to the circuit model result. For each curve, the impedance matrix was truncated with a different number of significant figures before solving the system of equations. The higher the number of significant figures, the better the result is. However, the method doesn't work below 1 MHz, even if the number of significant figures is increased to 9.

III. LOOP-TREE BASIS FUNCTION METHOD

The construction of the loop-tree basis functions starts from the physical decomposition of current

$$\mathbf{J} = \mathbf{J}^s + \mathbf{J}^i \qquad (2)$$

where $\mathbf{J}^s$ is the solenoidal current and $\mathbf{J}^i$ is the irrotational component. The loop basis functions are used to expand $\mathbf{J}^s$ and the tree basis functions for $\mathbf{J}^i$.

A loop basis function is associated with an inner node and its surrounding edges. Explicitly, the definition in terms of RWG basis functions is [2]

$$\mathbf{O}_n(\mathbf{r}) = \sum_{i \in \text{loop } n} \frac{\sigma_i}{l_i} \mathbf{f}_i(\mathbf{r}) \qquad (3)$$

where $\mathbf{f}_i$ is the RWG basis function for the ith edge connected to node n. l_i is the length of the edge and the coefficient $\sigma_i = \pm 1$ forces the current to flow in the same direction around node n. A tree basis function is simply chosen from a subset of the RWG basis functions and is complementary to the loop basis functions. The loop and tree basis functions form a complete set in the RWG space. It is easy to show that the loop basis function is divergence-free. Physically, that means there is no charge associated with the loop basis function.

The loop-tree basis function scheme inherently replaces the numerical integration of $\nabla\Phi$ over closed paths with the exact value of zero and preserves the information contained in A. The new basis function is a superposition of conventional rooftop basis functions. The new testing integral is a superposition of the original testing integrals so the matrix solution is preserved. However, to take this advantage of this technique, one has to identify all possible closed paths in the
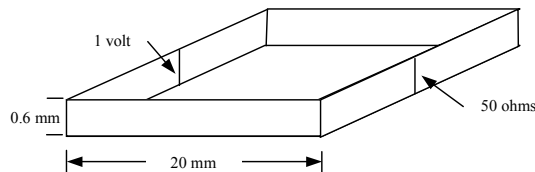

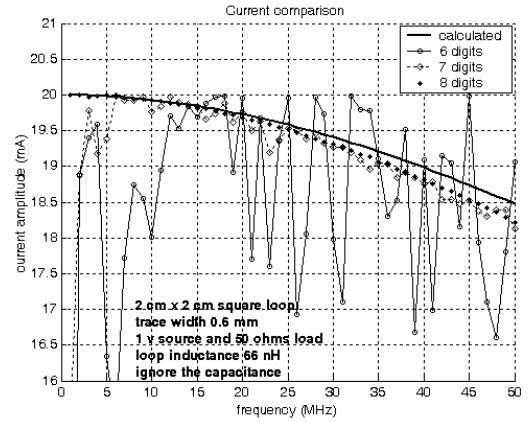
Figure 1. The geometry of a square loop

Figure 2. The current through the resistor

mesh. This requires searching the mesh to locate the inner nodes, identifying shared edges for each inner node, and adjusting the basis functions associated with the edges to orient them properly. This procedure can be quite complicated [2].

IV. LU RECOMBINATION METHOD

The new method we propose modifies the matrix equation using LU decomposition. This idea is based on the fact that the loop basis functions are constructed as linear combinations of the RWG basis functions and the tree basis functions are individual RWG functions that are complementary to the loop basis [5].

Consider the following $N \times N$ matrix equation

$$\mathbf{C} \cdot \mathbf{J} = \mathbf{F} \qquad (4)$$

obtained after applying the method of moments using RWG basis and testing functions. $\mathbf{C} = [C_{mn}]$ is an $N \times N$ matrix and $\mathbf{J} = [J_n]$ and $\mathbf{F} = [F_m]$ are column vectors of length N. The elements of $\mathbf{C}$ and $\mathbf{F}$ are given by [8]

$$
\begin{aligned}
C_{mn} &= C_{1mn} + C_{2mn} \\
&= -jk\eta \int_{S_m} \mathbf{f_m}(\mathbf{r}) \cdot \left[\int_{S_n} \mathbf{f_n}(\mathbf{r'}) \mathbf{G}_0(\mathbf{r}, \mathbf{r'}) dS' \right] dS \\
&\quad + j\frac{\eta}{k} \int_{S_m} \mathbf{f_m}(\mathbf{r}) \cdot \left[\int_{S_n} (\nabla' \cdot \mathbf{f_n}(\mathbf{r'})) \nabla' \mathbf{G}_0(\mathbf{r}, \mathbf{r'}) dS' \right] dS
\end{aligned}
\qquad (5)
$$

$$F_m = \int_{S_m} \mathbf{f_m}(\mathbf{r}) \cdot \left[\hat{n} \times \mathbf{E}^{inc}(\mathbf{r}) \right] dS \qquad (6)$$

where k is the wave number and η is the intrinsic impedance. $\mathbf{J}$ is the equivalent surface current density, and

$$\mathbf{G}_0(\mathbf{r}, \mathbf{r'}) = \frac{e^{-jk|\mathbf{r}-\mathbf{r'}|}}{4\pi|\mathbf{r}-\mathbf{r'}|} \qquad (7)$$

is the free space Green's function. Here the integral is a principal-value integral in which the singularity at $r = r'$ is excluded.

The function f_n is the RWG basis function. An important property of these functions is that the surface divergence, which is proportional to the surface charge density, is

$$\nabla \bullet f_n = \begin{cases} + l_n / A_n^+ & r \text{ in } T_n^+ \\ - l_n / A_n^- & r \text{ in } T_n^- \end{cases} \quad (8)$$

where l_n is the length of the nth edge and $A_n^{\pm}$ the area of the plus or minus triangle $T_n^{\pm}$ [1].

Comparing (1) and (5), it is clear that C_{1mn} corresponds to the vector potential while C_{2mn} corresponds to the scalar potential. As indicated previously, the matrix $\mathbf{C}_2$ is a singular matrix if closed loops exist. We can also prove this mathematically. First we write the elements of $\mathbf{C}_2$ as

$$
\begin{aligned}
C_{2mn} = & j\frac{\eta}{k}\int_{T_m^+}(\nabla \bullet f_m)\left[\int_{T_n^+}(\nabla' \bullet f_n)\mathbf{G}_0(r,r')dS'\right]dS \\
& + j\frac{\eta}{k}\int_{T_m^-}(\nabla \bullet f_m)\left[\int_{T_n^+}(\nabla' \bullet f_n)\mathbf{G}_0(r,r')dS'\right]dS \\
& + j\frac{\eta}{k}\int_{T_m^+}(\nabla \bullet f_m)\left[\int_{T_n^-}(\nabla' \bullet f_n)\mathbf{G}_0(r,r')dS'\right]dS \\
& + j\frac{\eta}{k}\int_{T_m^-}(\nabla \bullet f_m)\left[\int_{T_n^-}(\nabla' \bullet f_n)\mathbf{G}_0(r,r')dS'\right]dS
\end{aligned}
\quad , (9)
$$

and define

$$I(i,j) = \int_{T_i}\left[\int_{T_j}\mathbf{G}_0(r,r')dS'\right]dS . \quad (10)$$

Combining (8), (9) and (10), yields

$$
C_{2mn} = j\frac{\eta}{k}
\begin{bmatrix}
\left(\dfrac{l_m}{A_m^+}\right)\left(\dfrac{l_n}{A_n^+}\right)I(m^+,n^+) \\[2ex]
+\left(-\dfrac{l_m}{A_m^-}\right)\left(\dfrac{l_n}{A_n^+}\right)I(m^-,n^+) \\[2ex]
+\left(\dfrac{l_m}{A_m^+}\right)\left(-\dfrac{l_n}{A_n^-}\right)I(m^+,n^-) \\[2ex]
+\left(-\dfrac{l_m}{A_m^-}\right)\left(-\dfrac{l_n}{A_n^-}\right)I(m^-,n^-)
\end{bmatrix}.
\quad (11)
$$

Suppose there is an inner node surrounded by 4 triangles, T_a, T_b, T_c, and T_d. The edges shared by these four triangles are edges 1, 2, 3 and 4, as shown in Fig. 3. For simplicity, the orientations of the edges are defined to be counterclockwise.
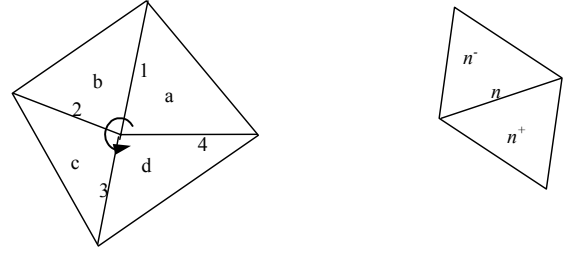

Figure 3.   Source and observation triangles

Now consider the integrals for these observation edges and a source edge n. We can write C_{21n}, C_{22n}, C_{23n}, and C_{24n} in the form of (11). It is easy to show that

$$\frac{C_{21n}}{l_1} + \frac{C_{22n}}{l_2} + \frac{C_{23n}}{l_3} + \frac{C_{24n}}{l_4} = 0 . \quad (12)$$

If any of the orientations is defined in an opposite way, we can simply change the corresponding plus sign in (12) to minus and (12) still holds.

Since n can be any edge in the mesh, (12) means rows 1, 2, 3, and 4 of the $\mathbf{C}_2$ matrix are linearly dependant. So if there is an inner node in the mesh, the row elements in the $\mathbf{C}_2$ matrix associated with the edges connecting to this inner node are linearly dependant and the $\mathbf{C}_2$ matrix is singular.

Comparing (12) to (3), we see how the singularity property of $\mathbf{C}_2$ is related to the loop basis function. Each of the loop-tree basis functions can be viewed as a linear combination of the RWG basis functions. Thus the testing on the loop-tree basis function is also a linear combination of the testing on the rooftop basis functions. That is to say, the matrix based on the loop-tree basis function set can be obtained from the matrix based on the rooftop basis functions by linear transformation. The purpose of the transformation is to find the closed loops and eliminate the integral of $\nabla\Phi$ on the loop. LU decomposition is a kind of linear transformation. After the decomposition, the matrix can be written as the product of a lower triangular matrix, $\mathbf{L}$, and an upper triangular matrix, $\mathbf{U}$. If the matrix is a singular matrix, $\mathbf{U}$ is also a singular matrix which has zeros on its diagonal.

We have shown that the matrix $\mathbf{C}_2$ resulting from the scalar potential is a singular matrix. That is, there should be at least one zero component on the diagonal of its $\mathbf{U}$ matrix. In the numerical computation, however, this zero is always a small, non-zero value due to the limited precision of the numerical computation. As the frequency goes lower, the unbalance between $\mathbf{C}_1$ and $\mathbf{C}_2$ is larger. So this non-zero value can become relatively large compared to the elements of $\mathbf{C}_1$. If we sum $\mathbf{C}_1$ and $\mathbf{C}_2$, we lose the information in $\mathbf{C}_1$ and are left with the numerical errors in $\mathbf{C}_2$.

We calculated two $\mathbf{C}_2$ matrices for a same example but with different computation accuracy and compared the $\mathbf{U}$ matrices. After carefully examining the elements, we found that most of the elements were nearly the same except for the values very near zero. The more accurate the computation was, the smaller

these values were. Thus, the errors accumulated in these near-zero values. Since we know the exact value of these elements, we can simply set them to zero. Moreover, since these values near zero imply the associated row is linearly dependant on other rows, the entire row should be zero.

Setting those rows to zero is the same as eliminating the contribution of $\nabla\Phi$ from the closed loops in the loop-tree basis function method. However, we don't need to explicitly create these loops in the mesh.

We summarize our LU recombination method here.

- Do the LU decomposition on the $\mathbf{C}_2$ matrix.

- Find the near-zero elements on the diagonal of $\mathbf{U}$ matrix.

- If these elements are not at the end of the $\mathbf{U}$ matrix, rearrange the $\mathbf{C}_2$ matrix and do the LU decomposition again.

- Set the near-zero rows of the $\mathbf{U}$ matrix to zero

- Construct a new $\mathbf{C}_2$ matrix with $\mathbf{L}$ and the new $\mathbf{U}$ matrix.

After the new $\mathbf{C}_2$ matrix is created, we can continue with the conventional algorithm to solve the problem.

V. NUMERICAL RESULTS

Fig. 4 shows the modeled results for the loop example in Fig. 1 using our proposed method. After the LU recombination, the boundary element solution is accurate down to 100 Hz without significant error.

Fig. 5 shows the results for a smaller (3 × 3 mm) loop example with a dense mesh. Note that the x axis is now a logarithmic scale. There were 4 inner nodes in this new mesh, so an additional permutation step was taken to set all four near-zero elements to zero. The figure shows the results from 1 kHz to 1 GHz. In fact, an accurate solution was obtained down to 1 Hz for this example.
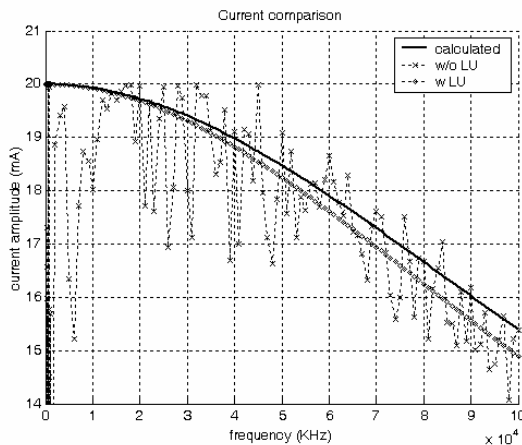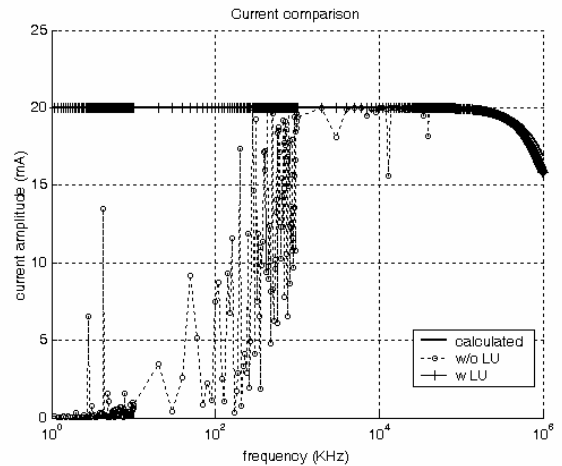

Figure 5. The current in a smaller loop modeled with and without LU recombination

VI. CONCLUSION

In this paper we present an LU recombination method to remove the low frequency instability inherent in the boundary element method using rooftop basis functions. This new method uses a linear transformation of the impedance matrix to find the dependent component in the integration of the scalar potential. This approach has the same effect as using a set of loop-tree basis functions. It accurately accounts for the cancellation over closed loops and preserves the information from the vector potential that otherwise would be lost due to numerical error.

REFERENCES

[1] S. M. Rao, D. R. Wilton, and A. W. Glisson, "Electromagnetic scattering by surfaces of arbitrary shape," *IEEE Trans. Antennas Propagat.*, vol. AP-30, No. 3, pp. 409-418, May 1982.

[2] M. Burton, S. Kashyap, "A study of recent moment-method algorithm that is accurate to very low frequencies," *Appl. Computational Electromagn. Soc. J.*, vol. 10, no. 3, pp. 58-68, Nov. 1995.

[3] W. Wu, A. W. Glisson, and D. Kajfez, "A study of two numerical solution processsdures for the electric field integral equation at low frequency," *Appl. Computational Electromagn. Soc. J.*, vol. 10, no. 3, pp. 69-80, Nov. 1995.

[4] J. R. Mautz and R. F. Harrington, "An E-field solution for a conducting surface small or comparable to the wavelength," *IEEE Trans. Antennas Propagat.*, vol. AP-32, pp. 330-339, Apr. 1984.

[5] S. Y. Chen, W. C. Chew, J. M. Song, and J. S. Zhao, "Analysis of low frequency scattering from penetrable scatterers," *IEEE Trans. Geoscience and Remote sensing*, vol. 39, no. 4, Apr. 2001.

[6] Y. H. Zhang, T. J. Cui, W. C. Chew, and J. S. Zhao, "Magnetic field integral equation at very low frequencies," *IEEE Trans. Antennas Propagat.*, vol. 51, no. 8, Aug. 2003.

[7] A. F. Peterson, S. L. Ray, and R. Mittra, "Computational methods for electromagnetics," New York: IEEE Press, 1997.

[8] Y. Ji, "Development and applications of a hybrid finite-element method/method-of-moments (FEM/MOM) tool to model electromagnetic compatibility and signal integrity problems in printed circuit boards," Ph.D. dissertation, University of Missouri-Rolla, 2000.

Figure 4. The current in a square loop modeled with and without LU recombination